Recovering Lost 21cm Radial Modes via Cosmic Tidal Reconstruction

Hong-Ming Zhu,[1,2] Ue-Li Pen,[3,4,5] Yu Yu,[6] and Xuelei Chen[1,2,7]

[1] *Key Laboratory for Computational Astrophysics, National Astronomical Observatories, Chinese Academy of Sciences, 20A Datun Road, Beijing 100012, China*
[2] *University of Chinese Academy of Sciences, Beijing 100049, China*
[3] *Canadian Institute for Theoretical Astrophysics, 60 St. George Street, Toronto, Ontario M5S 3H8, Canada*
[4] *Canadian Institute for Advanced Research, CIFAR Program in Gravitation and Cosmology, Toronto, Ontario M5G 1Z8, Canada*
[5] *Perimeter Institute for Theoretical Physics, 31 Caroline St. N., Waterloo, ON, N2L 2Y5, Canada*
[6] *Key laboratory for research in galaxies and cosmology, Shanghai Astronomical Observatory, Chinese Academy of Sciences, 80 Nandan Road, Shanghai 200030, China*
[7] *Center of High Energy Physics, Peking University, Beijing 100871, China*

(Dated: January 5, 2016)

21cm intensity mapping has emerged as a promising technique to map the large scale structure of the Universe, at redshifts z from 1 to 10. Unfortunately, many of the key cross correlations with photo-z galaxies and the CMB have been thought to be impossible due to foreground contamination for radial modes with small wavenumbers (copied). These modes are usually subtracted in the foreground subtraction process. We recover lost 21cm radial modes via cosmic tidal reconstruction and find more than 60% cross correlation signal at $\ell \lesssim 100$ and even more on larger scales can be recovered from null. The tidal reconstruction method opens up a new set of possiblities to probe our Universe and is extremely valuable not only for 21cm surveys but also CMB and photometric redshift observations.

PACS numbers:

Introduction.—The current and future cosmological observations aim to map a large fraction of the Universe with unprecedent precision, varying from LSST [1], Euclid [2][3], Planck mission (which paper shall we cite?), CMB S4 (cite which?), etc. In addition to these experiments, 21cm intensity mapping has emerged as a powerful probe of the large scale structure of the Universe [4][5]. However, the astrophysical foregrounds from galatic and extra-galatic synchrotron and free-free emissions are stronger than the cosmological 21cm signal by many orders of magnitude. These foregrounds are expected to be spectrally smooth, which means they would contaminate small radial modes, i.e. all modes with low $k_\parallel$. While there are not many modes with small $k_\parallel$, many other cosmic observations with broad window functions along the radial direction only probe these modes, like weak lensing, photo-z galaxies, integrated Sachs-Wolf effect, kinetic Sunyaev-Zel'dovich effect and others. Thus this makes it very hard to cross correlate these cosmic probes with 21cm intensity mapping surveys [6][7] (cite more?). To study how to solve this problem is of great importance for both 21cm intensity mapping surveys and other impartant cosmic surveys.

Recently an new method called *cosmic tidal reconstruction* has been developed [8][9], it can reconstruct the large scale tidal field and hence large scale density field from the alignment of small scale cosmic structures. The modes with small $k_\parallel$ and large $k_\perp$ are well reconstructed [9], which are exactly those lost in the foreground subtraction in 21cm experiments. This technique enables the reconstruction of small radial modes, which are essential for CMB and other cross correlations.

In this *L*etter we study how to use cosmic tidal reconstruction to reconstruct the lost large scale radial modes, and further cross correlate with CMB lensing, photo-z galaxies and ISW effect. We find such reconstruction technique recovers more than 60% cross correlation signal at $\ell \lesssim 100$ from nothing and even more at larger scales. This opens up a new set of possiblities to understand the origin and evolution of our Universe.

Cosmic tidal reconstruction.—Cosmic tides is a new way to view the tidal effect of gravity on the structure of matter clustering [8]. The large scale density field can be reconstructed from the anisotropic tidal distortions of the locally measured matter power spectrum with good accuracy [8][9]. The basic idea of purely transverse tidal reconstruction has been studied in Ref. [8] and further expanded in Ref. [9]. Here we briefly discuss the physical idea and summarize the process of cosmic tidal reconstruction.

The evolution of small scale density perturbations is modulated by long wavelength perturbations [10]. The anisotropic distortions in the local small scale power specturm, $\propto \hat{k}^i\hat{k}^j t_{ij}^{(0)}$, arise from the coupling of small scale density fluctuations with the large scale tidal field t_{ij}, where $t_{ij} = \Phi_{,ij} - \delta_{ij}\nabla^2\Phi/3$, $\hat{}$ denotes the unit vector and superscript (0) denotes some "initial" time. While in principle the tidal field t_{ij} has 5 independently observable components, the two transverse shear terms, $(\hat{k}_1^2 - \hat{k}_2^2)\gamma_1^{(0)}$ and $2\hat{k}_1\hat{k}_2\gamma_2^{(0)}$, which describe quadrupolar distortions in the tangential plane perpendicular to the line of sight, are less affected by peculiar velocities. Since $\gamma_1 = (\Phi_{,11} - \Phi_{,22})/2$ and $\gamma_2 = \Phi_{,12}$ only involves derivatives in the tangential plane, the changes in γ_1 and γ_2 due to redshift space distortion are expected to be a second order effect. The two gravitational tidal shear fields γ_1 and γ_2 can be converted to the 2D convergence field, $\kappa_{2D} = (\Phi_{,11} + \Phi_{,22})$, using

$$\kappa_{2D,11} + \kappa_{2D,22} = (\gamma_{1,11} - \gamma_{1,22} + 2\gamma_{2,12}). \qquad (1)$$

The 3D convergence $\kappa_{3\mathrm{D}} = \nabla^2\Phi/3 \propto \delta$ which gives the large scale density field, can further be obtained from

$$\kappa_{3\mathrm{D},11} + \kappa_{3\mathrm{D},22} = \frac{2}{3}\nabla^2\kappa_{2\mathrm{D}}. \tag{2}$$

Since only two transverse tidal shear fields $\gamma_1(\boldsymbol{x})$ and $\gamma_2(\boldsymbol{x})$ are used, the change of the large scale density field along the line of sight is inferred from the variations of γ_1 and γ_2 along the z axis. The error of $\kappa_{3\mathrm{D}}$ is

$$\sigma_{\kappa_{3\mathrm{D}}}(\boldsymbol{k}) \propto \left(k^2/k_\perp^2\right)^2, \tag{3}$$

which is anisotropic in $k_\perp$ and $k_\parallel$ [9]. The reconstruction works best for modes with low $k_\parallel$ and high $k_\perp$, which can not be obtained from 21cm surveys and contribute substantially to cosmological observables from other surveys mentioned above. Thus cosmic tidal reconstruction provides a good opportunity to recover lost radial modes and improve the cross correlations.

The tidal reconstrtion works as follows. The first step is to convolve the density field with a Gaussian kernel, $S(\boldsymbol{k}) = e^{-k^2R^2/2}$, which filters out the small scale nonlinear structures. Here we still take $R = 1.25$ Mpc$/h$ [8][9]. Next step is to gaussianize the smoothed density field by taking a logarithmic transform or ranking the density fluctuations into a Gaussian distribution. In the following reconstruction, we adopt the latter as after the simulated foreground subtraction, some of the density contrasts becomes smaller than -1, which makes it hard to take the logarithmic transform, $\ln(1+\delta)$. The gravitational tidal shear fields can be estimated by applying quadratic tidal shear estimators $\hat{\gamma}_1$ and $\hat{\gamma}_2$ to the density field as in 21cm lensing reconstruction [11]. Then the 3D tidal convergence field $\kappa_{3\mathrm{D}}$ is given by the linear combination of tidal shear fields using Eq.(1) and Eq.(2). The reconstructed noisy field $\kappa_{3\mathrm{D}}$ is related to the original density field as

$$\kappa_{3\mathrm{D}}(k_\perp, k_\parallel) = b(k_\perp, k_\parallel)\delta(k_\perp, k_\parallel) + n(k_\perp, k_\parallel), \tag{4}$$

where $b = P_{\kappa_{3\mathrm{D}}\delta}/P_\delta$ is the bias factor and n is the noise of reconstruction [9]. The reconstructed clean field is given by

$$\hat{\kappa}_c = (\kappa_{3\mathrm{D}}/b)W, \tag{5}$$

where the Wiener filter $W(k_\perp, k_\parallel) = P_\delta/(P_{\kappa_{3\mathrm{d}}}/b^2)$.

Simulation setup.—We further explore this idea with numerical simulations. We employ an ensemble of six N-body simulations from the CUBEP^{3}M code [12]. Each simulation includes 2048^3 particles in a $(1.2\mathrm{Gpc}/h)^3$ box with following cosmological parameters: Hubble parameter $h = 0.678$, baryon density $\Omega_b = 0.049$, dark matter density $\Omega_c = 0.259$, amplitude of primordial curvature power spectrum $A_s = 2.139 \times 10^{-9}$ at $k_0 = 0.05$ Mpc^{-1} and scalar spectral index $n_s = 0.968$. In the following analysis we use outputs at $z = 1$.

We could approximately use dark matter to represent 21cm source distributions. This is a good approximation since the neutral hydrogen traces the total mass distribution fairly well

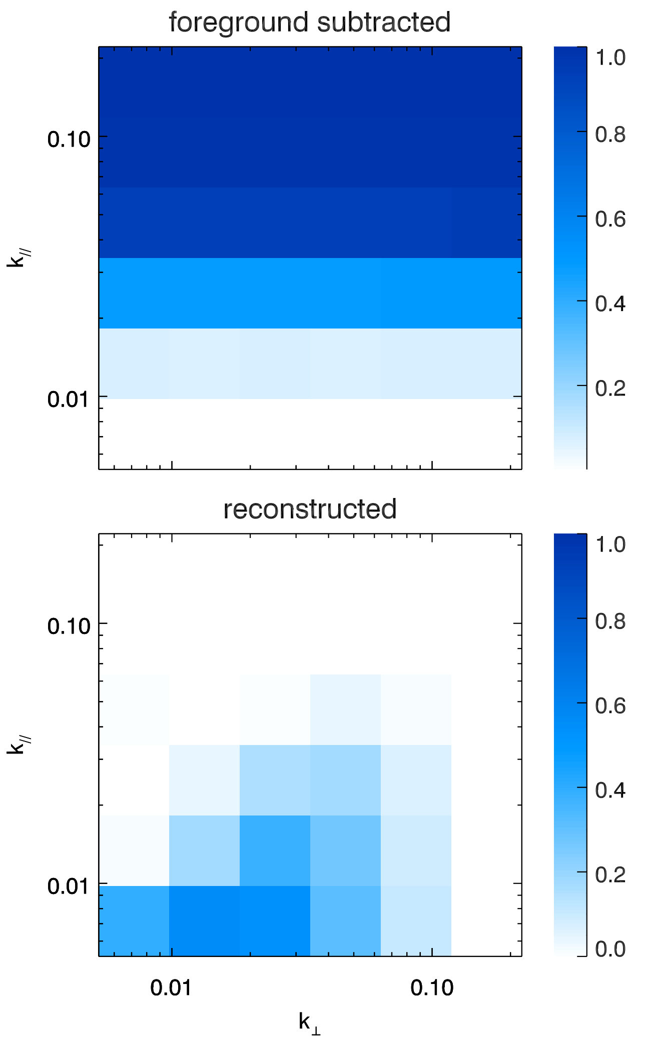

FIG. 1: The upper panel shows the ratio between the power spectra of the foreground subtracted density field and the original density field, i.e. $P_{\delta fs}/P_\delta$. The lower panel shows the ratio between the power spectra of the reconstructed field and the original density field, i.e. P_{κ_c}/P_δ. Here we show results for $R_\parallel = 60$ Mpc$/h$.

at low redshifts. We simply assume the experimental noise to be zero above a cut off scale and infinity below the cut off scale. This is a reasonable approximation for a filled aperture experiment, which has good brightness sensitivity and an exponetially growing noise at small scales. (above two sentences copied) We choose this scale to be $k_c = 0.5\ h/$Mpc, which corresponds to $\ell = 1150$ at $z = 1$. This is realistic for the ongoing 21cm experiments like CHIME [13][14] and Tianlai [15][16].

We are not going to provide a detailed 21cm data reduction process in this letter, so we simply use a high pass filter $W_{fs}(k_\parallel) = 1 - e^{-k_\parallel^2 R_\parallel^2/2}$ to simulate the foreground subtraction. We show results for the two different scales $R_\parallel = 60$ Mpc$/h$ and $R_\parallel = 15$ Mpc$/h$, which gives $W_{fs} = 0.5$ at $k_\parallel = 0.02$ Mpc$/h$ and $k_\parallel = 0.08$ Mpc$/h$, respectively. The former is an optimal case, i.e. we remove modes for

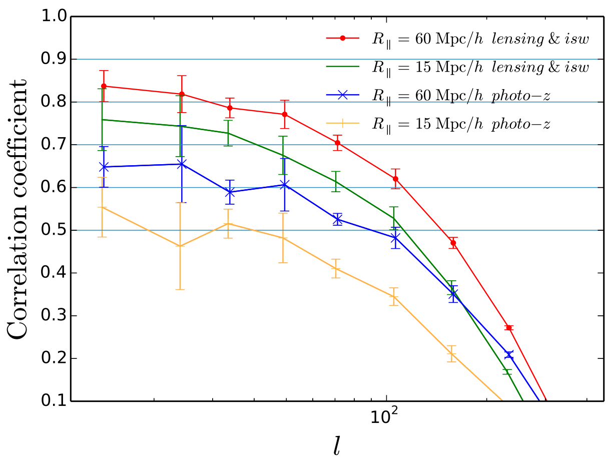

FIG. 2: Cross correlation coefficients.

$k_\parallel \lesssim 0.02$ Mpc/h while the latter is already achieved in the current 21cm observations [17][18].

The observed 21cm field after foreground subtraction is given by

$$\delta_{fs}(\boldsymbol{k}) = \delta(\boldsymbol{k}) W_{fs}(k_\parallel)\Theta(k_c - k), \tag{6}$$

where $\delta(\boldsymbol{k})$ is the density field from simulations, W_{fs} accounts the effect from foreground subtraction and $\Theta(x)$ is the step function which equals 1 for $x \geq 0$ and otherwise 0. Then we get the reconstructed clean field κ_c from δ_{fs} via cosmic tidal reconstruction. In Fig.1, the upper panel shows the ratio between $P_{\delta_{fs}}$ and P_δ and the lower panel shows the ratio between P_{κ_c} and P_δ for $R_\parallel = 60$ Mpc/h. We find the lost radial modes appears again in the reconstructed field.

Cross correlation signal.—To show how much the cross correlations is improved by cosmic tidal reconstruction and study the dectability of the cross correlations, we need to generate the lensing convergence field, the angular distribution of photo−z galaxies and the temperature fluctuation due to the ISW effect from N-body simulations.

(1) CMB lensing.—The weak lensing convergence is a weighted projection of the dark matter fluctuation along line-of-sight to the last scatter surface,

$$\kappa(\boldsymbol{\theta}) = \int_0^{\chi_s} d\chi W(\chi)\delta(\chi\boldsymbol{\theta}, \chi)\ , \tag{7}$$

where the lensing kernel

$$W(\chi) = \frac{3}{2}\Omega_{m0} H_0^2 a^{-1} \chi \frac{\chi_s - \chi}{\chi_s}\ , \tag{8}$$

with $\chi_s = \chi(z_s = 1090)$. To generate the convergence field from simulation data, we first squeeze the simulation box to a 2D plane, then multiply the $W(\chi)$, as the lensing weight is a slow varying function for the case of CMB lensing. Then we obtain the 2D convergence field contributed by the simulated density.

(2) Photometry survey.—We calculate the projected galaxy density field at $z \sim 1$ with usual photo-z bin width of 0.2, i.e. $z^P \in (0.9, 1.1)$. We adopt the galaxy distribution characterized by $n^P(z^P)dz^P \propto z^{P,\alpha}\exp[-(z^P/z^*)^\beta]$ with $\alpha = 2$, $z^* = 0.5$, $\beta = 1$ and assume the photo-z scatter $P(z^P|z)$ is perfectly known to be in a Gaussian form with photo-z error $\sigma_P = 0.05(1+z)$. The 2D angular galaxy distribution is given by

$$\delta_{2\mathrm{D}}(\boldsymbol{\theta}) = \int_0^\infty dz W(z)\delta(\chi\boldsymbol{\theta}, \chi(z))\ , \tag{9}$$

where the window function

$$W(z) = \int_{0.9}^{1.1} P(z^P|z) n^P(z^P) dz^P\ . \tag{10}$$

(3) ISW effect.—ISW is the observed CMB temperature fluctuations induced by the integral of the late-time potential variation

$$\frac{\Delta T}{T}(\boldsymbol{\theta}) = 2\int \dot{\Phi}(\boldsymbol{\theta}, t)dt\ . \tag{11}$$

In Fourier space, approximating that the evolution of the overdensity field with time is given by linear theory $\dot{\delta}(\boldsymbol{k}, t) = \dot{D}(t)\delta(\boldsymbol{k}, t=0)$, we have

$$\dot{\Phi}(\boldsymbol{k}, t) = \frac{3}{2}\Omega_{m0}\frac{H_0^2}{k^2}\frac{\delta(\boldsymbol{k}, t)}{a(t)}H(t)(1-\beta(t))\ , \tag{12}$$

where $\beta(t) = d\ln D(t)/d\ln a(t)$ and $D(t)$ is the growth factor. In our implementation, we also approximate the $\beta(t)$ as a constant across the simulation box.

In Fig. 2, we show the cross correlation coefficients for 21cm with different observations for both $R_\parallel = 60$ Mpc/h and $R_\parallel = 15$ Mpc/h. Due to the similar treatment of CMB lensing field and the ISW field, we get the same correlation coefficient for them. The correlation coefficient for photo-z galaxies is smaller than the other two since we use a narrow bin which locates at $z = 1$ with bins width 0.2.

In Fig. 3, we show the three cross correlation signals and the noise levels for the signal (is the green curve called noise level?). The error on the signal is given by

$$\sigma_{C_\ell} = \frac{1}{(2\ell+1)\Delta_\ell f_{\mathrm{sky}}}(C_\ell^{\alpha\beta})^2 + (C_\ell^\alpha + n_\ell^\alpha)(C_\ell^\beta + n_\ell^\beta) \tag{13}$$

For the 21cm field, $n_\ell^{21\mathrm{cm}}$ is given through Eq.(5). The noise for CMB lensing is assumed to be the same as *Planck* 2015 results [19]. For ISW effect, n_ℓ^{ISW} is the large scale CMB power spectrum C_ℓ^{TT}. We choose f_{sky} to be 0.25 for CMB lensing and photo-z galaxies, and 1 for the ISW effect. We find by using cosmic tidal reconsruction, we are able to detect the cross correlation signals with ongoing 21cm experiments [13–16]. The redshift information contained in 21cm observations allows us to constrain the expansion history of the Universe by cross correlating with the ISW effect. The detectability for ISW effect can be further improved by including CMB polarization data [20].

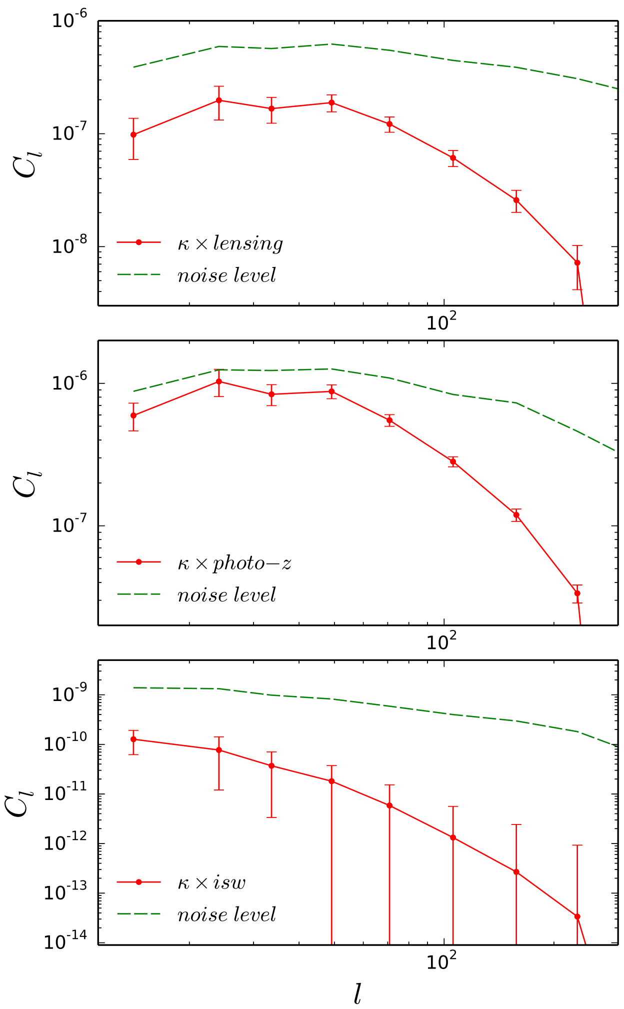

FIG. 3: The cross correlation signal between 21cm and other cosmic probes for $R_{\parallel} = 60$ Mpc/h.

Discussion.—It may seem to be odd that the modes lost appear again after reconstruction. This can be undertanded intuitively. The reconstructed field κ_c is given by the linear combination of quadratic estimators, in the form of $\kappa_c(\boldsymbol{x}) \sim \delta_{fs}(\boldsymbol{x})\delta_{fs}(\boldsymbol{x})$. In Fourier space this can be written as $\kappa_c(\boldsymbol{k}) \sim \int d^3k'\delta_{fs}(\boldsymbol{k}')\delta_{fs}(\boldsymbol{k}-\boldsymbol{k}')$, i.e. the reconstructed field is given by the convolution of $\delta_{fs}(\boldsymbol{k}')$ and $\delta_{fs}(\boldsymbol{k}-\boldsymbol{k}')$. Although δ_{fs} has no small radial nodes, i.e. $k'_{\parallel}$ and $k_{\parallel} - k'_{\parallel}$ can not be small, $k_{\parallel}$ can reach the low $k_{\parallel}$ regime. Here we extract the information about matter distribution on large scales contained in the small scale matter distributions. The power spectrum of κ_c is give by the connected four point function of δ_{fs}, which means we are using the information that comes from higher order statistics and is not included in the two point statistics of δ_{fs}, i.e. power spectrum.

The tidal shear estimators used is optimal for Gaussian sources and in the long wavelength limit [9]. The results can still be improved by constructing optimal tidal shear estimators for non-Gaussian sources as in 21cm lensing [21] and considering the general case. This means here we present the “least optimal” case of recovering the cross correlation signals and even better results can be achieved in future.

The BAO reconstruction technique [22] has been shown to be still useful in 21cm surveys [23][24]. While there are not many modes with small $k_{\parallel}$ lost in the foreground subtraction, the differential motions which smear the BAO peaks are substantially contributed by large scale modes with $k \lesssim 0.1\ h/\mathrm{Mpc}$ [22]. The tidal reconstruction compensates the foreground wedge at low $k_{\parallel}$ and high $k_{\perp}$ and hence can further improve the BAO reconstruction in 21cm surveys. Since all cosmological 21cm experiments share the same foreground problem, no matter low redshift surveys for BAO or high redshift observations for the EOR signal, the tidal reconstruction can also help high redshift cross correlations like the 21cm-kSZ signal from EOR [25]. Based on above discussions, we conclude that cosmic tidal reconstruction is extremely valuable for all cosmological 21cm surveys as well as CMB and photometric redshift observations.

We acknowledge helpful discussions with Marcelo Alvarez, Alex van Engelen, Philippe Berger, Yi-Chao Li and Shifan Zuo. Our simulation computations were performed on the BlueGene/Q supercomputer located at the University of Torontos SciNet HPC facility. SciNet is funded by the CFI under the auspices of Compute Canada, the Government of Ontario, the Ontario Research Fund Research Excellence; and the University of Toronto. We acknowledge the support of the Chinese MoST 863 program under Grant No. 2012AA121701, the CAS Science Strategic Priority Research Program XDB09000000, the NSFC under Grant No. 11373030 and 11403071, IAS at Tsinghua University, CHEP at Peking University, and NSERC.

[1] LSST Science Collaboration, P. A. Abell, J. Allison, S. F. Anderson, J. R. Andrew, J. R. P. Angel, L. Armus, D. Arnett, S. J. Asztalos, T. S. Axelrod, et al., ArXiv e-prints (2009), 0912.0201.

[2] R. Laureijs, J. Amiaux, S. Arduini, J. . Augères, J. Brinchmann, R. Cole, M. Cropper, C. Dabin, L. Duvet, A. Ealet, et al., ArXiv e-prints (2011), 1110.3193.

[3] L. Amendola, S. Appleby, D. Bacon, T. Baker, M. Baldi, N. Bartolo, A. Blanchard, C. Bonvin, S. Borgani, E. Branchini, et al., Living Reviews in Relativity **16**, 6 (2013), 1206.1225.

[4] T.-C. Chang, U.-L. Pen, J. B. Peterson, and P. McDonald, Physical Review Letters **100**, 091303 (2008), 0709.3672.

[5] T.-C. Chang, U.-L. Pen, K. Bandura, and J. B. Peterson, Nature **466**, 463 (2010), 1007.3709.

[6] S. R. Furlanetto and A. Lidz, ApJ **660**, 1030 (2007), astro-ph/0611274.

[7] P. J. Adshead and S. R. Furlanetto, MNRAS **384**, 291 (2008), 0706.3220.

[8] U.-L. Pen, R. Sheth, J. Harnois-Deraps, X. Chen, and Z. Li, ArXiv e-prints (2012), 1202.5804.

[9] H.-M. Zhu, U.-L. Pen, Y. Yu, X. Er, and X. Chen, ArXiv e-prints (2015), 1511.04680.

[10] F. Schmidt, E. Pajer, and M. Zaldarriaga, Phys. Rev. D **89**, 083507 (2014), 1312.5616.

[11] T. Lu and U.-L. Pen, MNRAS **388**, 1819 (2008), 0710.1108.

[12] J. Harnois-Déraps, U.-L. Pen, I. T. Iliev, H. Merz, J. D. Emberson, and V. Desjacques, MNRAS **436**, 540 (2013), 1208.5098.

[13] K. Bandura, G. E. Addison, M. Amiri, J. R. Bond, D. Campbell-Wilson, L. Connor, J.-F. Cliche, G. Davis, M. Deng, N. Denman, et al., in *Society of Photo-Optical Instrumentation Engineers (SPIE) Conference Series* (2014), vol. 9145 of *Society of Photo-Optical Instrumentation Engineers (SPIE) Conference Series*, p. 22, 1406.2288.

[14] L. B. Newburgh, G. E. Addison, M. Amiri, K. Bandura, J. R. Bond, L. Connor, J.-F. Cliche, G. Davis, M. Deng, N. Denman, et al., in *Society of Photo-Optical Instrumentation Engineers (SPIE) Conference Series* (2014), vol. 9145 of *Society of Photo-Optical Instrumentation Engineers (SPIE) Conference Series*, p. 91454V, 1406.2267.

[15] X. Chen, International Journal of Modern Physics Conference Series **12**, 256 (2012), 1212.6278.

[16] Y. Xu, X. Wang, and X. Chen, ApJ **798**, 40 (2015), 1410.7794.

[17] K. W. Masui, E. R. Switzer, N. Banavar, K. Bandura, C. Blake, L.-M. Calin, T.-C. Chang, X. Chen, Y.-C. Li, Y.-W. Liao, et al., ApJ **763**, L20 (2013), 1208.0331.

[18] E. R. Switzer, K. W. Masui, K. Bandura, L.-M. Calin, T.-C. Chang, X.-L. Chen, Y.-C. Li, Y.-W. Liao, A. Natarajan, U.-L. Pen, et al., MNRAS **434**, L46 (2013), 1304.3712.

[19] Planck Collaboration, P. A. R. Ade, N. Aghanim, M. Arnaud, M. Ashdown, J. Aumont, C. Baccigalupi, A. J. Banday, R. B. Barreiro, J. G. Bartlett, et al., ArXiv e-prints (2015), 1502.01591.

[20] G.-C. Liu, K.-W. Ng, and U.-L. Pen, Phys. Rev. D **83**, 063001 (2011), 1010.0578.

[21] T. Lu, U.-L. Pen, and O. Doré, Phys. Rev. D **81**, 123015 (2010), 0905.0499.

[22] D. J. Eisenstein, H.-J. Seo, E. Sirko, and D. N. Spergel, ApJ **664**, 675 (2007), astro-ph/0604362.

[23] H.-J. Seo and C. M. Hirata, ArXiv e-prints (2015), 1508.06503.

[24] J. D. Cohn, M. White, T.-C. Chang, G. Holder, N. Padmanabhan, and O. Doré, ArXiv e-prints (2015), 1511.07377.

[25] M. A. Alvarez, ArXiv e-prints (2015), 1511.02846.